http://dx.doi.org/10.5012/bkcs.2014.35.4.1133

Rapid Screening of Phospholipid Biomarker Candidates from Prostate Cancer Urine Samples by Multiple Reaction Monitoring of UPLC-ESI-MS/MS and Statistical Approaches

Sangsoo Lim,[†] Dae Young Bang,[†,‡] Koon Ho Rha,[§,*] and Myeong Hee Moon[†,*]

[†]*Department of Chemistry, Yonsei University, Seoul 120-749, Korea. [*]E-mail: mhmoon@yonsei.ac.kr*
[‡]*Lotte R&D Center, Seoul 150-194, Korea*
[§]*Department of Urology, Yonsei University College of Medicine, Seoul 120-752, Korea. [*]E-mail: khrha@yuhs.ac*
Received September 27, 2013, Accepted December 22, 2013

Ultrahigh performance liquid chromatography-electrospray ionization-tandem mass spectrometry (UPLC-ESI-MS/MS) provides a high-speed method to screen a large number of samples for small molecules with specific properties. In this study, UPLC-ESI-MS/MS with multiple reaction monitoring (MRM) was employed to screen urinary phospholipid (PL) content for biomarkers of prostate cancer. From lists of urinary PLs structurally identified using nanoflow LC-ESI-MS/MS, 52 PL species were selected for quantitative analysis in urine samples between 22 cancer-free urologic patients as controls and 45 prostate cancer patients. Statistical treatment of data by receiver operating characteristic (ROC) analysis yielded 14 PL species that differed significantly in relative concentrations (area under curve (AUC) > 0.8) between the two groups. Among PLs present at higher levels in prostate cancer urine, phosphatidylcholines (PCs) and phosphatidylinositols (PIs) constituted the major head group PLs (3 PCs and 7 PIs). For technical reasons, PL species of low abundance may be underrepresented in data from UPLC-ESI-MS/MS performed in MRM mode. However, the proposed method enables the rapid screening of large numbers of plasma or urine samples in the search for biomarkers of human disease.

Key Words : Lipidomics, Prostate cancer, Phospholipid biomarkers, UPLC-ESI-MS/MS, ROC analysis

Introduction

Prostate cancer is the most common cancer among men in the developed world, and tends to develop in men over the age of fifty. Rates of prostate cancer detection vary worldwide.[1,2] Prostate cancer diagnosis is based on symptoms, tissue biopsy, and measurements of prostate-specific antigen (PSA) in blood. While the PSA test is the most common screening implement for the disease, a reliable method is still needed, since the PSA test is in some case unreliable.[3]

An ideal biomarker for prostate cancer would be a molecular species involved in the early steps of carcinogenesis. Use of mass spectrometry (MS) in the proteomic or metabolomic analysis of human urine has yielded annexin A3[4] and basic human urinary arginine amidase[5] as protein markers, and sarcosine[6] as a metabolic marker of the disease. Lipids have attracted interest in the search for biomarkers because of their structural diversity and complexity and involvement in hormonal signaling, particularly through the regulation of membrane receptors that mediate interactions between cells. Lipid composition largely governs the structure and function of cell membranes.[7] Precisely because lipids are structurally complex and diverse, a lipidomics study must begin with a comprehensive characterization of the lipid content of the material of interest. Useful technologies for lipid analysis include nuclear magnetic resonance (NMR) spectroscopy,[8,9] Raman spectroscopy,[10] gas chromatography-mass spectrometry (GC-MS),[11,12] and electrospray ionization-mass spectrometry (ESI-MS).[13,14] However, liquid chromatography-ESI-tandem mass spectrometry (LC-ESI-MS/MS) in particular facilitates lipidomic analysis in separating complicated lipid mixtures with subsequent soft ionization of lipid molecules without preliminary modification and in deriving structural information from fragments of target ions.[15-17] Several classes of mammalian lipids have been examined as biological indicators for various diseases, including Alzheimer's disease,[18] pancreatic cancer,[19] mitochondrial dysfunction,[20] breast cancer,[21] coronary artery disease (CAD),[22] and prostate cancer.[23] Urinary PLs between prostate cancer patients and healthy controls were examined by using nLC-ESI-MS/MS in our earlier study,[24] however due to the relatively low speed it was limited to analyze small number of samples.

This study investigated potential urinary phospholipid biomarkers of prostate cancer using ultrahigh performance LC-ESI-MS/MS (UPLC-ESI-MS/MS) with statistical analysis. Initially, 52 urinary PL species, found greater than the limit of quantitation of method applied in present study and identified by structural determination using nanoflow LC/ESI-MS/MS in the previous study[25] were selected for the high speed screening of a large number of urine samples with prostate cancer. The current study was expanded to urologic patient groups (22 cancer-free urologic patients including benign prostate hyperplasia as controls in com-

parison to 45 prostate cancer patients) and quantitation was made by using multiple reaction monitoring (MRM) of fragment ions using UPLC/ESI-MS/MS. Quantitative data for potential PL biomarkers were screened for significance using receiver operating characteristic (ROC) analysis, a widely used biomarker discovery tool[26-29] that measures selectivity and sensitivity simultaneously.

Experimental

Materials and Reagents. Twenty phospholipid standards (12:0-LPC (lysophosphatidylcholine), 16:0-LPC, 14:0-LPE (lysophosphatidyl ethanolamine), 18:0-LPE, 12:0/12:0-PC (phosphatidylcholine), 16:0/14:0-PC, 16:0/16:0-PC, 18:0/18:1-PC, 20:0/20:0-PC, 12:0/12:0-PE, 16:0/16:0-PE, 18:0/18:0-PE, 18:0-LPA (lysophosphatidic acid), 18:0-LPG (lysophosphatidylglycerol), 18:0-LPS (lysophosphatidyl-serine), 18:1-LPI (lysophosphatidylinositol), 16:0/16:0-PA, 14:0/14:0-PG, 18:0/18:0-PS and 16:0/18:2-PI) were purchased from Avanti Polar Lipids (Alabaster, AL, USA) to establish optimal separation conditions, cone voltage, and MS collision energy for each different PL head group in UPLC-ESI-MS-MS analysis. Formic acid, ammonium hydroxide, and chloroform were all MS grade and were obtained from Sigma (St. Louis, MO, USA). Solvents used for UPLC-ESI-MS experiments (water, acetonitrile, methanol, and isopropanol) were all HPLC grade and were purchased from Avantor Performance Materials (Phillipsburg, NJ, USA).

Urine Samples and Lipid Extraction. Sixty-seven patients were selected from the Institutional Review Board (IRB) database. Urine samples were collected from 22 cancer-free urologic patients with conditions that included benign prostate hyperplasia as controls and from 45 prostate cancer patients who visited Severance Hospital, Yonsei University College of Medicine (Seoul, Korea) from 2011 to 2012. The cancer patient urine samples were collected just before prostatectomy, and the control samples were obtained after fasting. Data for controls and patients (Table 1) show significant differences between the two groups in PSA level. Subjects in the control group were overweight (body mass index (BMI) 25.0-29.9) and cancer patients were of normal or subnormal body weight (BMI < 25). Urine samples were stored at −20 °C immediately after collection until lipid extraction.

Lipids were extracted from human urine as previously described[30] with modifications. Briefly, 5 mL of each urine sample was transferred to a 15 mL centrifuge tube, and the tube was wrapped with MilliWrap from Merck Millipore (Billerica, MA, USA). Tubes thus prepared were placed under liquid nitrogen for rapid freezing and lyophilized for 12 hours in a vacuum centrifuge from Ilshin Biobase Co. (Yangju, Korea). Recovered sediment was reconstituted with 4.5 mL of $CHCl_3$:CH_3OH (2:1) solution containing spiked phospholipids, 13:0/13:0-PC and 15:0/15:0-PG, as internal standards for positive and negative ion modes in MS analysis, respectively, at final concentrations of 200 fmol/μL. Then, 900 μL of MS-grade water was added and the mixture was vortexed thoroughly. The mixture was centrifuged at 2500 rpm for 10 minutes and the lower organic layer was transferred to a new centrifuge tube and vacuum centrifuged for drying. The recovered lipids were reconstituted with CH_3OH:CH_3CN (9:1) solution to a final concentration of 100 μg/μL and stored at 4°C for the UPLC-ESI-MS/MS experiments.

UPLC-ESI-MS/MS. An ultrahigh performance liquid chromatography (UPLC) system coupled to a Xevo TQ mass spectrometer from Waters (Milford, MA, USA) was used to separate the complex mixture of extracted lipids, and the components were quantified using an analytical column, Xbridge C_{18} (3.5 μm, 2.1 × 50 mm) from Waters. From each urinary lipid extract, 1 μL was injected through an autosampler and separation was allowed to proceed at a fixed flow rate of 0.4 mL/min. A binary gradient elution was applied, with water for solvent A and 10/30/60 (v/v/v) methanol/acetonitrile/isopropanol for solvent B. Each mobile phase was supplemented, with 0.1% formic acid for positive ion mode and 0.05% ammonium hydroxide for negative ion mode to enhance ionization of PLs during MS. Quantification was made through the multiple reaction monitoring (MRM) component of MS/MS. All analyses described above, including lipid extraction, were repeated three times. Capillary voltage was set at 3.0 kV. Cone voltage, collision energy, and other experimental conditions for MRM analysis were adjusted for each PL depending on the type of polar head group (see Table 2). In a previous study,[31] class-specific daughter ions were used as quantifier ions for MRM; however, acyl chain-specific fragment ions were denoted as daughter ions for each class to distinguish the composition

Table 1. Demographic features of control subjects and patients with prostate cancer

	Control (n=20)	Patient					p-value (p *vs* c)
		Overall (n=43)	Gleason Score				
			6 (n=10)	7 (n=27)	8 (n=2)	9 (n=4)	
Age (yrs)	60.5 ± 15.2	64.6 ± 8.3	63.0 ± 7.2	63.7 ± 8.9	72.5 ± 2.1	68.8 ± 6.1	0.269
Height (cm)	168.8 ± 6.6	167.5 ± 5.3	165.6 ± 5.7	168.5 ± 5.4	166.5 ± 7.8	166.7 ± 2.6	0.446
Weight (kg)	68.3 ± 8.2	68.2 ± 7.3	65.7 ± 5.6	69.5 ± 8.1	61.0 ± 5.7	70.0 ± 3.6	0.963
BMI	27.9 ± 6.3	24.3 ± 2.0	24.0 ± 1.5	24.5 ± 2.2	22.0 ± 0.0	25.2 ± 1.4	0.021
PSA	3.3 ± 6.8*	9.0 ± 5.7	9.2 ± 3.1	8.6 ± 4.6	9.6 ± 0.0	9.7 ± 15.4	0.003

of the two acyl chains. The peak area of each species was calculated by MassLynx from Waters, and the peak area ratio of target species was calculated relative to the area of an internal standard at each ion mode (13:0/13:0-PC for positive ion and 15:0/15:0-PG for negative ion mode).

Statistical Methods. Specificities and sensitivities for ROC curve generation, as well as precision and F-measure generation values, were calculated by establishing diverse threshold values using Microsoft Excel. Student's t-test was performed for each PL candidate using Minitab 15 (www.minitab.co.kr). Final selection of PL markers from screening was based on the following threshold criteria: more than a 3-fold difference between control and patient groups, p-value less than 0.01, and area under the curve (AUC) of more than 0.8.

Results and Discussion

Figure 1 shows the base peak chromatograms of a) twelve PL standards and b) urinary lipid extracts of a cancer-free control (hereafter as control) and a prostate cancer patient sample (hereafter patient sample) with IS added (13:0/13:0-PC) in positive ion mode. Figure 1(a) demonstrates that PL standards can be separated in less than 8 minutes by UPLC-ESI-MS with sufficient resolution to separate LPL regioisomers: peaks 1a and 1b in the enlarged chromatogram represent lyso/12:0-PC and 12:0/lyso-PC, respectively. During each UPLC-ESI-MS/MS run of urinary extract, 52 target PL species were quantitatively analyzed by calculating the peak area of each daughter ion (quantifier ion) obtained by the MRM method. These 52 target PL molecules were selected for analysis from among the 85 species of urinary PLs that

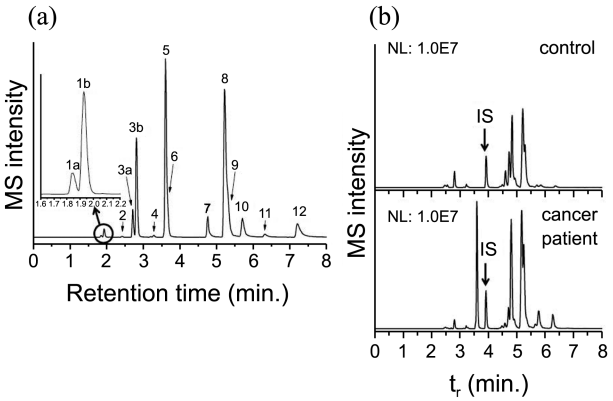

Figure 1. Base peak chromatograms (BPCs) of (a) 12 PL standards and (b) lipids extracted from urine samples of a cancer-free control patient and a prostate cancer patient using nLC-ESI-MS/MS with an IS (13:0/13:0-PC). Standard PLs were 1. 12:0-LPC (1a for lyso/12:0-PC and 1b for 12:0/lyso-PC), 2. 14:0-LPE, 3. 16:0-LPC, 4. 18:0-LPE, 5. 12:0/12:0-PC, 6. 12:0/12:0-PE, 7. 14:0/16:0-PC, 8. 16:0/16:0-PC. 9. 16:0/16:0-PE, 10. 18:0/18:0-PC, 11. 18:0/18:0-PE, and 12. 20:0/20:0-PC.

we previously identified and characterized using nLC-ESI-MS/MS.[25] The quantifier ions used for each PL group selected were the fragment ions obtained by loss of an acyl chain (sn-1 for diacyl PLs) from each parent ion as $[M+H-RCOOH]^+$ for the LPC, PC, PE, and LPE groups, and the free carboxylate ion, $[RCOO]^-$, for PS, PI, LPS, PG, PA, and LPA groups. The *m/z* values of the precursor ion and the corresponding daughter ion of each PL species are listed in Table 2 along with their corresponding molecular chain structures. For the head group of each PL species, cone voltage and collision voltage were separately controlled. For

Table 2. List of targeted PL groups and the corresponding MS/MS conditions adjusted for the type of head group. Molecular species examined in MRM mode during UPLC-ESI-MS/MS and their characteristic *m/z* values for precursor ions and quantifier ions are listed

	Cone/ Collision Voltage (V)	Type of precursor/ quantifier ions	Molecular Species (*m/z* of precursor/quantifier ions)
LPC (3)	35 / 30	$[M+H]^+$/ $[M+H-RCOOH]^+$	14:0/lyso (468/240), lyso/18:2 (520/240), 16:0/lyso (496/240)
LPE (4)	25 / 20		lyso/20:4 (502/224), 20:4/lyso (454/224), 16:0/lyso (480/224), 18:1/lyso (482/224)
PC (12)	35 / 30		16:0/22:6 (806/550), 16:0/20:4 (782/526), 18:2/18:2 (782/502), 16:0/18:2 (758/502), 18:0/20:5 (808/524), 18:1/18:2 (784/502), 16:0/16:0 (734/478), 16:0/18:1 (760/504), 18:0/20:4 (810/526), 18:1/18:1 (786/504), 18:0/18:2 (786/502), 18:0/18:1 (788/504)
PE (10)	25 / 20		16:0/22:6 (764/508), 16:0/20:4 (740/484), 18:1/20:4 (766/484), 16:0/18:2 (716/460), 18:1/18:2 (742/460), 16:0/18:1 (718/462), 18:1/18:1 (744/462), 18:0/18:2 (744/460), 18:0/20:4 (768/484), 18:0/18:1 (746/462)
LPS (1)	35 / 30	$[M-H]^-$/ $[RCOO]^-$	lyso/18:0 (524/283)
LPA (2)	42 / 24		lyso/16:0 (409/255), lyso/18:0 (437/283)
PS (5)	53 / 45		16:0/18:1 (760/255), 18:0/20:4 (810/283), 18:1/18:1 (786/281), 18:0/18:2 (786/283), 18:0/18:1 (788/283)
PI (11)	75 / 45		16:0/20:4 (857/255), 16:0/20:3 (859/255), 18:0/20:4 (885/283), 16:0/16:0 (809/255), 16:0/18:1 (835/255), 18:1/16:0 (835/281), 18:1/18:1 (861/281), 18:0/18:2 (861/283), 18:0/20:3 (887/283), 16:0/18:0 (837/255), 18:0/18:1 (863/283)
PG (2)	57 / 46		18:2/22:6 (817/279), 18:1/22:6 (819/281)
PA (2)	42 / 36		16:0/16:0 (647/255), 18:0/18:2 (699/283)

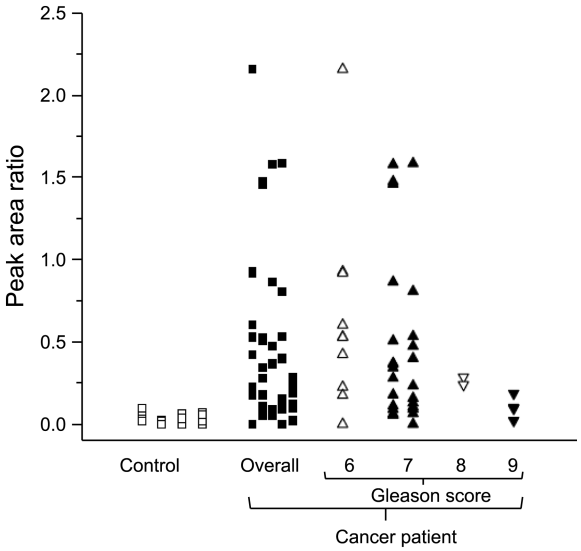

Figure 2. Plot of peak area ratio (*vs.* IS) of 16:0/18:0-PI from controls (n=20) and patients (n=43). Data for patient group are plotted by overall and by individual Gleason Scores (G=6, 7, 8, and 9).

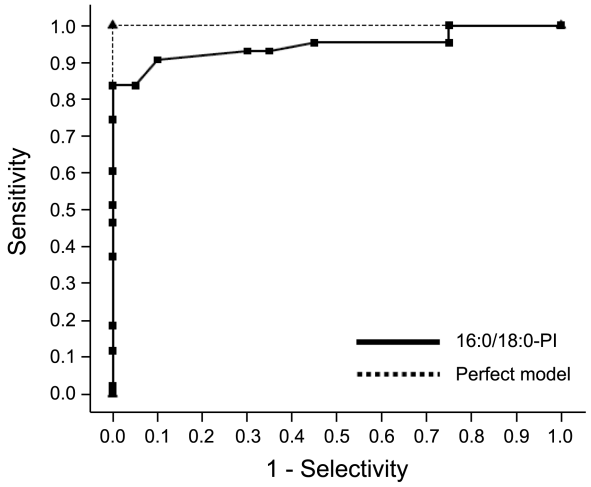

Figure 3. ROC curve of 16:0/18:1-PI species showing the correlation between sensitivity and 1-selectivity calculated at 17 threshold points. The dotted line represents the perfect model.

all 52 PL species, triplicate measurements were made for each urinary extract sample. Figure 2 shows an example of average relative peak area ratio (*vs.* IS) of 16:0/18:0-PI plotted for all control and cancer patient samples. Each patient sample was plotted two different ways: one for overall Gleason Score and the other for individual Scores. Gleason score is a system of grading ranging from 0 to 10 that support the prognosis of a person with prostate cancer with the greater score meaning the worse tumor prognosis. Basically, it is the sum of two individual numbers assigning 'primary grade' and 'secondary grade' of the tumor observed. Figure 2 shows a very broad distribution of the relative abundances of 16:0/18:0-PI species among cancer patients and a distribution among controls that is comparatively narrow. The coefficient of variation (CV) in triplicate measurements of each species was less than 5% (data not shown for each).

After calculating the average peak area ratio, Grubb's test, which is to find and eliminate possible outliers in a univariate data from a population conforming to the normal distribution, was applied to eliminate outliers. This revealed a significant difference within each control and patient group, resulting in the exclusion of two control samples and two patient samples from the original dataset prior to calculation of the abundance ratios (patient over control). The average relative peak area of each urinary PL for the control group (n=20) and the prostate cancer patient group (n=43) are listed in Table S1 of Supporting Information. Data for the patient group are expressed by overall and individual Gleason Scores (G=6 (n=10), 7 (n=27), 8 (n=2), and 9 (n=4)). Among the 52 species examined in this study, 32 molecular species differed significantly in relative peak area (greater than three-fold) between control and patient groups. To evaluate correlations with the presence or progression of prostate cancer, statistical calculations were applied for the first 32 PL species screened. A contingency table was established for each species to calculate the following parameters: sensitivity, selectivity (or specificity), precision, balanced accuracy, F-measure, and area under the ROC curve (AUC). To calculate statistical parameters for each PL species screened, 17 threshold values (or classifiers) of peak area ratio were selected; these thresholds were established at the medians and quartiles of each distribution (Figure 2). The numbers of samples within or out of each threshold value were counted to calculate true positive, false positive, false negative, and true negative rates, so as to calculate sensitivity (rate of declaring true positive values as true), selectivity (rate of declaring false positive as false), precision (rate of true counts to total counts that were declared as true), balanced accuracy ((sensitivity + selectivity)/2), and F-measure (harmonic mean of precision and sensitivity). The ROC curve in Figure 3 was generated by plotting sensitivity *vs.* (1-selectivity) calculated at all 17 threshold values for 16:0/18:0-PI (see Figure 2). The dotted line represents the perfect model. The area under the ROC curve (AUC) was calculated for each species. From these calculations, 14 PL species were selected from the 32 species based on the following criteria: AUC > 0.800, p/c ratio > 3.00, p-value < 0.01, sensitivity > 0.500 and balanced accuracy > 0.700. The final 14 PL species were divided into two classes (nine species for AUC > 0.900 and five species for 0.800 < AUC < 0.900; Table 3). Sensitivity and selectivity values shown for each species listed in Table 3 are the values yielding the maximum value of a sum (sensitivity + selectivity). In an earlier study, we demonstrated the use of nLC-ESI-MS/MS in a semi-quantitative analysis of urinary PL species from 9 prostate cancer patients and 10 healthy control subjects.[24] That study identified 10 potential prostate cancer biomarkers, *i.e.*, PL species showing greater than 3-fold difference in relative levels between patients and controls. In this study, several experimental conditions have been changed. These include the number of patient samples (n=43 for the present work *vs.* 9 for the previous one),

Table 3. List of potential PL biomarkers statistically selected by the following criteria: ratio (patient/control) > 3.00, p-value < 0.01, sensitivity > 0.500, balanced accuracy > 0.700, and AUC > 0.900 (for first nine species) and AUC > 0.800 (for the last five species)

	Lipid Species	Ratio (P/C)	p-value	Sens.	Selec.	Prec.	Balanced Accuracy	Inform.	MCC	F-measure	AUC
PC1	**18:1/18:1-PC**	6.69 ± 7.66	< 0.001	0.651	1.000	1.000	0.826	0.651	0.610	0.789	0.939
PC2	**16:0/16:0-PC**	5.52 ± 6.71	< 0.001	0.698	0.950	0.968	0.824	0.648	0.603	0.811	0.931
PC3	**18:0/18:1-PC**	7.49 ± 11.44	< 0.001	0.674	0.900	0.935	0.787	0.574	0.535	0.784	0.917
PI1	**16:0/18:0-PI**	14.23 ± 19.85	< 0.001	0.605	1.000	1.000	0.802	0.605	0.572	0.754	0.946
PI2	**16:0/20:3-PI**	7.40 ± 9.04	< 0.001	0.558	1.000	1.000	0.779	0.558	0.535	0.716	0.938
PI3	**18:0/18:2-PI**	6.19 ± 8.27	< 0.001	0.674	0.900	0.935	0.787	0.574	0.535	0.784	0.920
PI4	**18:0/20:3-PI**	5.96 ±7.12	< 0.001	0.698	0.950	0.968	0.824	0.864	0.603	0.811	0.919
PI5	**16:0/20:4-PI**	4.37 ± 6.64	< 0.001	0.535	0.950	0.958	0.742	0.485	0.465	0.687	0.912
PI6	**18:0/18:1-PI**	7.60 ± 9.89	< 0.001	0.698	0.950	0.968	0.824	0.648	0.603	0.811	0.901
PI7	**18:0/20:4-PI**	3.17 ± 3.15	< 0.001	0.698	0.750	0.857	0.724	0.448	0.419	0.769	0.877
PE1	**18:0/18:2-PE**	3.47 ± 3.81	< 0.001	0.651	0.850	0.903	0.751	0.501	0.467	0.757	0.866
LPE1	**16:0/lyso-PE**	4.48 ± 6.92	< 0.001	0.674	0.900	0.935	0.787	0.574	0.535	0.784	0.856
LPE2	**18:1/lyso-PE**	5.03 ± 7.96	< 0.001	0.651	0.850	0.903	0.751	0.501	0.467	0.757	0.849
LPS1	**lyso/18:0-PS**	5.35 ± 12.14	0.007	0.628	0.800	0.871	0.714	0.428	0.398	0.730	0.800

sample origin, quantification method (quantifier ion obtained in MRM mode *vs.* peak area measurement of precursor ion from extracted ion chromatogram), MS instrument type (triple quadrupole *vs.* ion trap), injected amount of PL extracts (100/100 μg *vs.* 15/5 μg for positive/negative ion modes), and LC columns and flow rate (0.4 mL/min *vs.* 300 nL/min) for ESI. In particular, the ionization efficiencies of PL in two ESI-MS experiments run at different flow rates may differ significantly, and thus, low abundance PL species counted as candidates in the previous run were not detected in the present study. Moreover, the present study compared the difference between prostate cancer patient samples and cancer-free urologic patients with benign prostate hyperplasia, while the former study focused on the difference in prostate cancer patients from healthy controls. Among the 10 selected PL species (excluding LPE and LPS) listed in Table 3, three PL species (18:1/18:1-PC, 18:0/18:1-PC, and 18:0/20:4-PI) were detected as high abundance species with significantly higher levels in cancer patient samples in both experiments. The p/c ratio for each species calculated was 6.69 ± 7.66 from UPLC-ESI-MS/MS (5.12 ± 2.09 from nLC-ESI-MS) for 18:1/18:1-PC, 7.49 ± 11.47 (3.26 ± 1.76) for 18:0/18:1-PC, and 3.17 ± 3.15 (5.97 ± 4.82) for 18:0/20:4-PI. While two other PL species (16:0/18:2-PC and 16:0/18:1-PI) showed significant increases (p/c > 4) in both experiments, these were not included in Table 3 since they did not meet the statistical thresholds applied in the present study.

Principal component analysis (PCA) was applied to the 14 selected species in Table 3, and the resulting plots are shown in Figure 4. The scores plot in the left of Figure 4 shows that points for cancer-free patient samples (filled circles) cluster at the upper left of the plot while the points (open circles) for the cancer patient group are widely scattered, indicating that relative amounts of these 14 species vary widely within the cancer group. The loading plot at the right side of Figure 4 shows the narrow distribution of 14 selected species (see x- and y-axis scales in comparison to those of the scores plot), indicating that the relative amounts of these species are significantly higher in cancer patients than in cancer-free controls.

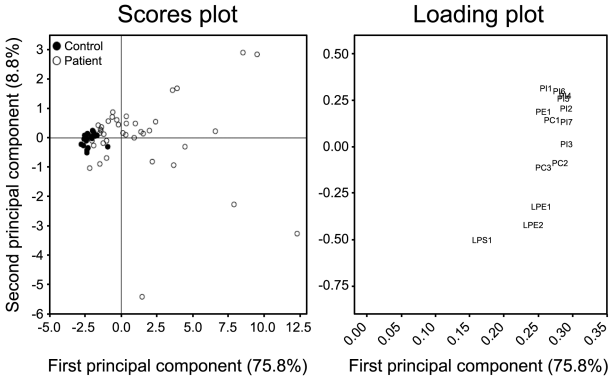

Figure 4. Principal component analysis (PCA) plots for the 14 selected PL species listed in Table 3. The narrow distribution of these 14 species in the loading plot at the right side (compare scales of the two axes) indicates that they are increased in the patient group.

Conclusion

This study demonstrated the utility of UPLC-ESI-MS/MS in the quantitative analysis of urinary phospholipids in an effort to develop biomarkers for prostate cancer. Complex urinary phospholipids were separated at high speed (10 min or less) by UPLC. Statistical analysis revealed significant quantitative differences in PL content between urine samples from prostate cancer patients and control samples from cancer-free urologic patients. Based on this analysis of 20 control and 43 prostate cancer samples, patients with prostate cancer may excrete several PL species at significantly higher concentrations than do subjects of comparable age

who do not have prostate cancer but with benign prostate hyperplasia. Among the 14 PL species detected at highest levels (AUC > 0.800) in prostate cancer, three PCs and seven PIs constitute major head groups. Increased level of PC in patients with prostate cancer is consistent with published data on the relative levels of PCs in samples of patients' plasma[23] and of PC in high-grade prostate cancer tissues.[32] In addition, 18:1/18:1-PC, 18:0/18:1-PC, and 18:0/20:4-PI were among the selected species found in our previous study to be significantly increased in patients with prostate cancer compared to healthy controls,[24] although experimental conditions in that study differed from those in the present one (see above).

A limitation of the present study is the difficulty of detecting low-abundance PL species and some head groups (PS and PA) which are not favorably ionized if there is spectral congestion under the relatively high feeding flow rate used in UPLC-ESI-MS/MS compared with nLC-ESI-MS/MS. Given the small number of samples in this study, the validity of the selected PL species as biomarkers is uncertain. However, the current study demonstrates the capability of UPLC-ESI-MS/MS to systematically screen large numbers of samples for molecular species with selected properties. These same features may be applied in the search for biomarkers of other significant adult diseases, including breast cancer and atherosclerosis.

Acknowledgments. This study was supported by grant NRF-2012-005598 from the National Research Foundation of Korea.

References

1. Siegel, R.; Ward, E.; Brawley, O.; Jemal, A. *CA Cancer J. Clin.* **2011**, *61*, 212.
2. Baade, P. D.; Youlden, D. R.; Krnjacki, L. J. *Mol. Nutr. Food Res.* **2009**, *53*, 171.
3. Brawley, O. W. *Seminars and Original Investigations* **2004**, *22*, 353.
4. Gerke, V.; Creutz, C. E.; Moss, S. E. *Nat. Rev. Mol. Cell Biol.* **2005**, *6*, 449.
5. Matsuda, Y.; Miyashita, A.; Fujimoto, Y.; Umeda, T.; Akihama, S. *Biol. Pharm. Bull.* **1996**, *19*, 1083.
6. Sreekumar, A.; Poisson, L. M.; Rajendiran, T. M.; Khan, A. P.; Cao, Q.; Yu, J.; Laxman, B.; Mehra, R.; Lonigro, R. J.; Li, Y.; Nyati, M. K.; Ahsan, A.; Kalyana-Sundaram, S.; Han, B.; Cao, X.; Byun, J.; Omenn, G. S.; Ghosh, D.; Pennathur, S.; Alexander, D. C.; Berger, A.; Shuster, J. R.; Wei, J. T.; Varambally, S.; Beecher, C.; Chinnaiyan, A. M. *Nature* **2009**, *457*, 910.
7. Orešič, M.; Hänninen, V. A.; Vidal-Puig, A. *Trends Biotechnol.* **2008**, *26*, 647.
8. Sotirhos, N.; Herslöf, B.; Kenne, L. *J. Lipid Res.* **1986**, *27*, 386.
9. Meneses, P.; Glonek, T. *J. Lipid Res.* **1988**, *29*, 679.
10. Wu, H.; Volponi, J. V.; Oliver, A. E.; Parikh, A. N.; Simmons, B. A.; Singh, S. *Proc. Natl. Acad. Sci. USA* **2011**, *108*, 3809.
11. Kuksis, A.; Myher, J. J.; Marai, L. *J. Am. Oil Chem. Soc.* **1984**, *61*, 1582.
12. Heller, D. N.; Murphy, C. M.; Cotter, R. J.; Fenselau, C.; Uy, O. M. *Anal. Chem.* **1988**, *60*, 2787.
13. Han, X.; Gross, R. W. *Mass Spectrom. Rev.* **2005**, *24*, 367.
14. Koivusalo, M.; Haimi, P.; Heikinheimo, L.; Kostiainen, R.; Somerharju, P. *J. Lipid Res.* **2001**, *42*, 663.
15. Taguchi, R.; Houjou, T.; Nakanishi, H.; Yamazaki, T.; Ishida, M.; Imagawa, M.; Shimizu, T. *J. Chromatogr. B* **2005**, *823*, 26.
16. Bang, D. Y.; Kang, D.; Moon, M. H. *J. Chromatogr. A* **2006**, *1104*, 222.
17. Lee, J. Y.; Min, H. K.; Moon, M. H. *Anal. Bioanal. Chem.* **2011**, *400*, 2953.
18. Sato, Y.; Nakamura, T.; Aoshima, K.; Oda, Y. *Anal. Chem.* **2010**, *82*, 9858.
19. Beger, R.; Schnackenberg, L.; Holland, R.; Li, D.; Dragan, Y. *Metabolomics* **2006**, *2*, 125.
20. Han, X.; Yang, J.; Cheng, H.; Yang, K.; Abendschein, D. R.; Gross, R. W. *Biochemistry (Mosc)* **2005**, *44*, 16684.
21. Glunde, K.; Jie, C.; Bhujwalla, Z. M. *Cancer Res.* **2004**, *64*, 4270.
22. Byeon, S. K.; Lee, J. Y.; Lim, S.; Choi, D.; Moon, M. H. *J. Chromatogr. A* **2012**, *1270*, 246.
23. Zhou, X.; Mao, J.; Ai, J.; Deng, Y.; Roth, M. R.; Pound, C.; Henegar, J.; Welti, R.; Bigler, S. A. *PLoS one* **2012**, *7*, e48889.
24. Min, H. K.; Lim, S.; Chung, B. C.; Moon, M. H. *Anal. Bioanal. Chem.* **2011**, *399*, 823.
25. Bang, D. Y.; Lim, S.; Moon, M. H. *J. Chromatogr. A* **2012**, *1240*, 69.
26. Mishra, J.; Dent, C.; Tarabishi, R.; Mitsnefes, M. M.; Ma, Q.; Kelly, C.; Ruff, S. M.; Zahedi, K.; Shao, M.; Bean, J.; Mori, K.; Barasch, J.; Devarajan, P. *The Lancet* **2005**, *365*, 1231.
27. Kozak, K. R.; Amneus, M. W.; Pusey, S. M.; Su, F.; Luong, M. N.; Luong, S. A.; Reddy, S. T.; Farias-Eisner, R. *Proc. Natl. Acad. Sci. USA* **2003**, *100*, 12343.
28. Kreisberg, J. I.; Malik, S. N.; Prihoda, T. J.; Bedolla, R. G.; Troyer, D. A.; Kreisberg, S.; Ghosh, P. M. *Cancer Res.* **2004**, *64*, 5232.
29. Bewick, V.; Cheek, L.; Ball, J. *Critical Care* **2004**, *8*, 1.
30. Folch, J.; Lees, M.; Stanley, G. H. S. *J. Biol. Chem.* **1957**, *226*, 497.
31. Xia, Y. Q.; Jemal, M. *Rapid Commun. Mass Spectrom.* **2009**, *23*, 2125.
32. Keshari, K. R.; Tsachres, H.; Iman, R.; Delos Santos, L.; Tabatabai, Z. L.; Shinohara, K.; Vigneron, D. B.; Kurhanewicz, J. *NMR Biomed.* **2011**, *24*, 691.